PHYSICAL REVIEW B VOLUME 36, NUMBER 2 15 JULY 1987-I

Structure and bonding of small semiconductor clusters

D. Tomanek
Department of Physics, University of California, Berkeley, and Center for Advanced Materials, Lawrence Berkeley Laboratory, Berkeley, California 94720

M. A. Schluter
AT&T Bell Laboratories, Murray Hill, New Jersey 07974
(Received 24 November 1986)

We calculate the geometrical and electronic structure of small Si_n, Si_n^+, and Si_n^- clusters up to sites $n=14$ within a combined tight-binding–density-functional-theory scheme. Especially stable structures for $n=6$ and 10 coincide with observed abundancies in the experimental mass spectra. All equilibrium structures are found to be close packed, with a different bonding than found in the bulk fragments. A transition to bulklike open structures is estimated to occur at cluster sizes $n \approx 10^2$–10^3.

I. INTRODUCTION

The properties of small atomic clusters have received much attention over the past decade.[1] These finite systems represent a new type of materials which show fingerprints of properties observed in atomic or molecular physics on one hand and condensed matter physics on the other hand. Also, the large portion of surface atoms makes small clusters interesting for applications in catalysis.[2] The low coordination of surface atoms causes bond contractions,[3] which have also been observed at extended surfaces of many systems. These bond contractions, which are large on the average and "tunable" through the cluster size, make small clusters behave as matter under high pressure and can lead to new structures. Finally, the pronounced size dependence of the electronic structure of small clusters is expected to lead to materials with mass-tailored optical and electrical properties.

So far, the largest portion of experimental effort has been devoted to cluster production. Clusters are produced in pulsed ultrasonic beams following a vapor condensation[4] or laser vaporization[5] and their size is usually determined in a mass analyzer after a charging and acceleration process. In contrast to this class of clusters produced in vacuum or in low-pressure carrier gas, clusters of quite well-defined sizes can also be grown in solution.[6,7]

In general, observed mass spectra do depend on cluster-preparation conditions, such as their charge state, temperature and cooling rate, and type and pressure of the carrier gas. Of special importance for the theoretical interpretation of the structure and bonding in small clusters are pronounced features such as abundant cluster sizes ("magic numbers") which do *not* depend on the preparation technique. At present, such mass spectra are available for rare gases, alkali metals, transition metals, semiconductors, and insulators.[1]

For elements whose cohesion is mainly due to nondirectional van der Waals interactions, such as rare-gas clusters, we expect the equilibrium structure to be close packed and stability maxima to occur at sizes corresponding to specially compact icosahedron arrangements at $n=13$, 55, 147, 309, etc.[4] For simple metals, which have been successfully described by the jellium approximation, the stability has been found to be mainly determined by the kinetic energy of electrons in a jellium droplet rather than the atomic postions.[8] Materials with covalent bonding, such as semiconductors, present a hybrid situation between these two cases. There, the strength of the directional covalent bonds depends on the atomic positions. While a strong surface tension due to many dangling bonds is expected to favor compact metallike structures at small cluster sizes, the increasing portion of bulklike atoms in larger clusters will finally induce a transition to more open crystal structures with reconstructed surfaces. The main objective of this investigation is to study the equilibrium structures and bonding in this class of materials, in our case represented by silicon. While the structure of bulk silicon has been thoroughly studied both experimentally and theoretically,[9] our study has been encouraged by recent photofragmentation experiments of small silicon clusters.[5] Our main results for the Si_n clusters have been published in a brief version elsewhere.[10] Some of our conclusions could also be compared to other calculations, which were performed by using different quantum-chemical methods.[11,12] After our calculation was completed, we became aware of a cluster calculation, which applies a formalism similar to the tight-binding part of our calculation to a limited number of Si clusters and arrives at similar conclusions.[13]

Our paper is structured as follows: In Sec. II we outline the theoretical approach we use to describe small semiconductor clusters. In Sec. III we apply this formalism to Si clusters and present results. The general conclusion and possible extensions of our study are summarized in Sec. IV.

II. THEORETICAL TOOLS

The study of small clusters imposes an additional problem to that encountered when investigating solid-state sys-

tems with many electrons. Successful approaches such as the local density approximation (LDA) have been developed,[14] but the calculation effort required limits their application to a small number of structures. While this is not a serious problem in solid-state systems, where the geometric structure is known in many cases, in small clusters the large number of configurational degrees of freedom for the ionic positions makes a true geometry optimization within the LDA virtually impossible.

We therefore choose a dual-track approach. We first use an empirical tight-binding (TB) method to presearch the $3n-6$ six-dimensional configuration space for possible equilibrium structures of an n atomic cluster. A limited number of geometries is then investigated more closely within the LDA.

The tight-binding method we use here is an extension of a Hamiltonian, which has been previously successfully applied to the reconstruction of semiconductor surfaces.[15] The cohesive energy of the cluster $E_{\rm coh}$ can be written as a sum of a band-structure energy $E_{\rm BS}$ and a repulsive energy E_R as

$$E_{\rm coh}=E_{\rm BS}+E_R \ . \tag{2.1}$$

The band-structure energy is given by

$$E_{\rm BS}=\sum_{\alpha} n_\alpha \varepsilon_\alpha - n\sum_{\beta} n^0_\beta \varepsilon^0_\beta + U\sum_{i=1}^{n}(q_i-q_i^0)^2 \ , \tag{2.2}$$

where the first two terms denote the one-electron energy of the cluster and n isolated atoms, respectively, and the third is an intra-atomic Coulomb interaction. In our notation, α and β correspond to electronic levels of the cluster and isolated atoms, respectively, and Roman indices denote sites. The electronic levels ε_α of the cluster are obtained from a tight-binding Hamiltonian of the form

$$H_{\rm TB}=\sum_i\sum_\beta \varepsilon^0_{i\beta} a^\dagger_{i\beta}a_{i\beta}+\sum_{\substack{i,j\\ i<j}}^{nn}\sum_{\beta,\beta'} t_{i\beta,j\beta'}(a^\dagger_{i\beta}a_{j\beta'}+\text{c.c.}) \ , \tag{2.3}$$

where $\varepsilon^0_{i\beta}$ are the atomic levels and $t_{i\beta,j\beta'}$ are parametrized nearest-neighbor hopping integrals. Net charge transfers $\Delta q_i=(q_i-q_i^0)$ at the atomic sites are obtained from a Mulliken population analysis. Structures with large Δq_i are effectively suppressed by the intra-atomic Coulomb interactions.

The repulsive energy E_R consists of pairwise interatomic interactions $E_r(d_{ij})$ and a term which only depends on the total number of bonds n_b and the number of atoms n in the cluster,

$$E_R=\sum_{\substack{i,j\\ i<j}} E_r(d_{ij})-n\left[\psi_1(n_b/n)^2+\psi_2(n_b/n)+\psi_3\right] \ . \tag{2.3}$$

The constants ψ_1,ψ_2, and ψ_3 are used to exactly reproduce cohesive energies of dimers and bulk structures with different coordination numbers, such as the diamond and bcc structures of silicon. For dimers, these coefficients are selected in such a way that

$$E_R^{\rm dimer}=E_r(d_{12}) \tag{2.5}$$

and $E_r(d)$ is *defined* as the difference of "exact" cohesive energy and a band-structure energy given by Eq. (2.2), as

$$E_r(d)\equiv E^{\rm dimer}_{\rm exact\ coh}(d)-E_{\rm BS}(d) \ . \tag{2.6}$$

To a good approximation, $E^{\rm dimer}_{\rm exact\ coh}$ can be obtained from *ab initio* calculations. For charged clusters, we only consider obvious changes in the band-structure term $E_{\rm BS}$ and keep E_R the same as for neutrals. In summary, the above described parametrization of our tight-binding energy formula is expected to produce a reasonable interpolation between dimers and selected bulk structures, which are reproduced exactly. Uncertainties remain as to the definition of a bond. Ideally, $E_{\rm BS}+E_R$ should be independent of this definition; however, the corrective term in (2.4) and the nearest-neighbor tight-binding Hamiltonian are too simple to achieve this. We choose to call $d\le d_c$ a bond, which introduces discontinuities at the saddle points of configurational energy surfaces.

In the density functional part of our calculation, we solve self-consistently the set of Kohn-Sham equations[16]

$$(-\tfrac{1}{2}\nabla^2+V_{\rm ion}+V_H+V_{\rm XC})\psi_\alpha=\varepsilon_\alpha\psi_\alpha \tag{2.7a}$$

and

$$\rho(\mathbf{r})=\sum_{\alpha}^{\rm occ}|\psi_\alpha(\mathbf{r})|^2 \tag{2.7b}$$

for a given cluster. $V_{\rm ion}$ is the external pseudopotential due to the ions. The Hartree potential V_H and the exchange-correlation potential $V_{\rm XC}$, which is used within the LDA form are both functionals of the charge density $\rho(\mathbf{r})$. For a self-consistent charge density corresponding to the electronic ground state, the total energy of the cluster can be obtained from

$$E_{\rm tot}=\sum_\alpha \varepsilon_\alpha-\tfrac{1}{2}\int V_H[\rho]\rho(\mathbf{r})d^3r + \int \rho(\mathbf{r})(\varepsilon_{\rm XC}[\rho]-V_{\rm XC}[\rho])d^3r+E_{\text{ion-ion}} \ , \tag{2.8}$$

where $\varepsilon_{\rm XC}[\rho]$ is the exchange-correlation energy density and $E_{\text{ion-ion}}$ is the electrostatic interaction energy among the bare pseudoions. The cohesive (or atomization) energy of an n atomic cluster is finally given by

$$E_{\rm coh}=E_{\rm tot}(\text{cluster})-nE_{\rm tot}(\text{isolated atom}) \ . \tag{2.9}$$

In the following section we use the combined TB-LDA formalism to obtain the equilibrium geometries, energies, and electronic structure of small Si clusters.

III. CALCULATIONS AND RESULTS FOR SMALL Si CLUSTERS

In the tight-binding calculation of Si, we use a four-state (s,p_x,p_y,p_z) Hamiltonian.[15] The diagonal elements are s- and p-level energies[15] $E_s=-5.25$ eV and $E_p=1.20$ eV, respectively. We use Slater-Koster parametrized[17] hopping integrals which show a $1/r^2$ distance dependence. Their values for $r=2.35$ Å, which is the bulk equilibrium nearest-neighbor distance, are[15] $V_{ss\sigma}=-1.938$ eV, $V_{sp\sigma}=1.745$ eV, $V_{pp\sigma}=3.050$ eV, and $V_{pp\pi}=-1.075$ eV. The corresponding band structure of Si in the diamond structure is shown in Fig. 1. We use

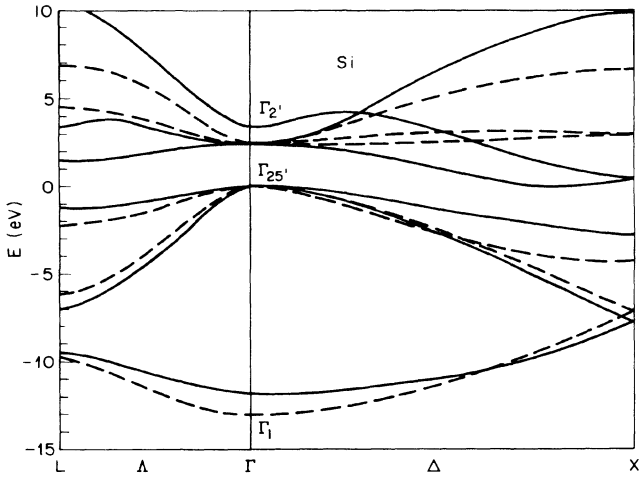

FIG. 1. Band structure of bulk Si obtained from the tight-binding Hamiltonian (dashed lines) and the density functional Hamiltonian (solid lines).

$U=1$ eV for the intra-atomic Coulomb interaction. The pairwise repulsive energy, defined by Eq. (2.6), is obtained by using the results of an *ab initio* configuration interaction (CI) calculation[18] for $E_{\rm coh}(Si_2)$ and is shown in Fig. 2. We used an analytic fit for the cohesive energy of Si_2, given by[18]

$$E_{\rm coh}(d)=A\,[(d/d^*)^p-(d/d^*)^q]\exp[\gamma/[a-(d/d^*)]^\nu]\ , \tag{3.1}$$

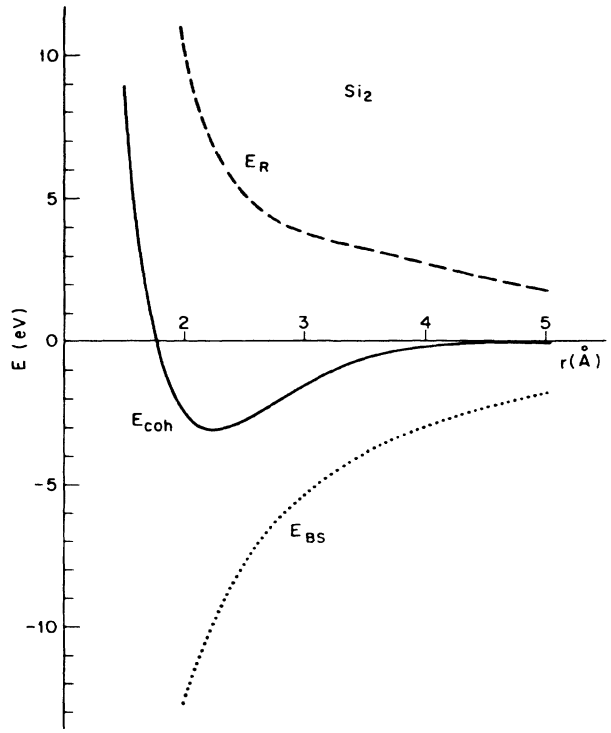

FIG. 2. Decomposition of the cohesive energy $E_{\rm coh}$ of Si_2 into the (tight-binding) band-structure energy E_{BS} and the repulsive energy E_R, plotted against internuclear distance.

where $A=80\,716.3$ eV, $d^*=1.781$ Å, $p=-3.372$, $q=-0.476$, $\gamma=-10.706$, $a=2.807$, and $\nu=0.310$. The TB calculation gives a very good representation of Si dimer properties: the bond length $d_0=2.27$ Å (expt. value of 2.24 Å), binding-energy $E_{\rm coh}=-3.07$ eV (expt. value of -3.0 eV), and vibration frequency $\omega_0=519$ cm^{-1} (expt. value of 511 cm^{-1}). In our nearest-neighbor Hamiltonian, the criterion for i and j being neighbors was that their distance $d_{ij}<2.55$ Å, which is the average of nearest- and second-nearest-neighbor distance in bulk Si, i.e., near the minimum in the radial distribution function. As mentioned above, this introduces some arbitrariness into the TB picture, since different nearest neighbor (nn) maps can lead to different energies for the same geometry, which could cause difficulties in the minimization procedure. For this reason, we choose nn maps and kept them fixed during geometry optimization.

In our calculation, degenerate levels have been populated in a symmetric way. Geometries with partially occupied degenerate levels at the "Fermi energy" are unstable with respect to static Jahn-Teller distortions. The constants used in the bond-number-dependent term in Eq. (2.4) are $\psi_1=0.225$ eV, $\psi_2=1.945$ eV, and $\psi_3=-1.03$ eV. These values set this term to zero for Si_2 and correctly reproduce *ab initio* cohesive energies[9] of bulk Si in the diamond structure $E_{\rm coh}=-4.64$ eV and in the bcc structure $E_{\rm coh}=-4.24$ eV. Also other bulk properties are reproduced quite well, such as for Si (diamond) the lattice constant $a_0=5.47$ Å (expt. value of 5.43 Å) and the bulk modulus $B=0.88$ a.u. (expt. value of 0.99 a.u.), and for the high-pressure phase Si(bcc) $a_0=3.25$ Å (calc. value of 3.12 Å).[9]

A useful help in the search for equilibrium geometries was the calculation of Hellman-Feynman forces, given by

$$F_i=-\frac{\partial E_{\rm tot}}{\partial r_i}=-\frac{\partial E_{\rm BS}}{\partial r_i}-\frac{\partial E_R}{\partial r_i},\quad i=1,\ldots,3n \tag{3.2a}$$

where

$$\frac{\partial E_{\rm BS}}{\partial r_i}=\sum_\alpha n_\alpha\frac{\partial}{\partial r_i}\langle\psi_\alpha\,|\,H\,|\,\psi_\alpha\rangle\approx\sum_\alpha n_\alpha\left\langle\psi_\alpha\left|\frac{\partial H}{\partial r_i}\right|\psi_\alpha\right\rangle\ . \tag{3.2b}$$

The structures corresponding to a minimum energy were found by using a minimization procedure, which started from different "seed" geometries for each cluster size. A selected number of structures was subsequently analyzed using the density functional formalism. The ionic potentials $V_{\rm ion}$ in Eq. (2.7a) were replaced by norm-conserving pseudopotentials of the Hamann-Schluter-Chiang type.[19] For the exchange-correlation functional we used the local form proposed by Ceperly and Alder.[20] Our basis consisted of local s, p, and d orbitals, which have been expanded in a Gaussian basis with two decays per orbital. Previously, this scheme reproduced plane-wave calculations of bulk Si properties with good accuracy.[21] Spin-polarization effects have been neglected in our calculation. They are expected to change the cohesive properties,[11] but not the nature of the bonding, the equilibrium structures, and the trends in the cohesive energy.

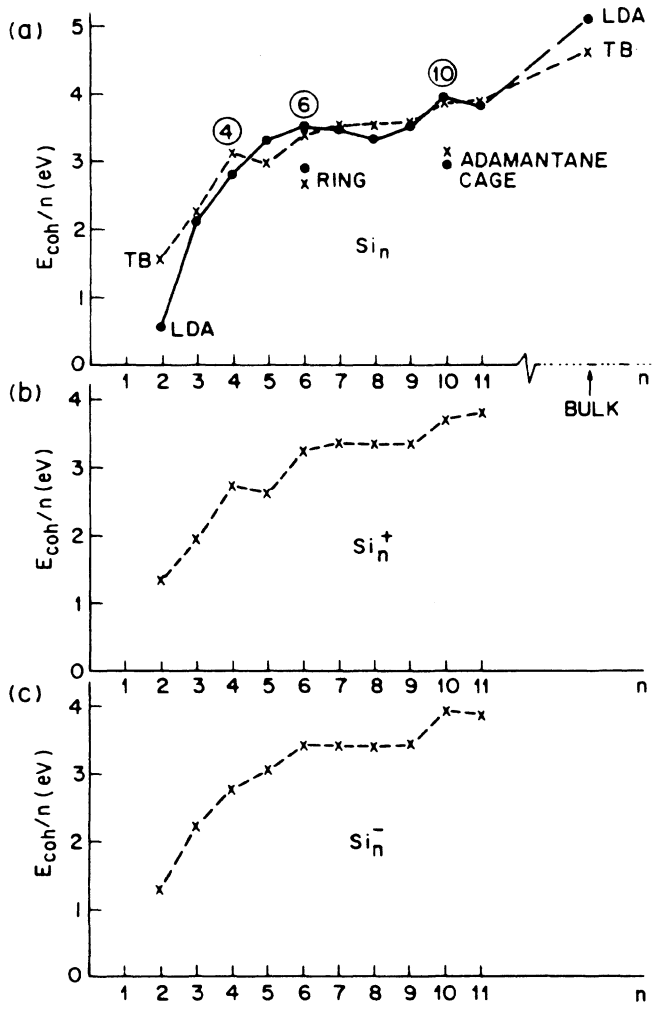

FIG. 3. Cohesive energy per atom of small Si_n, Si_n^+, and Si_n^- clusters. Tight-binding results are connected by a dashed line; local-density functional results are connected by a solid line.

In Fig. 3 we present results for the cohesion of Si_n, Si_n^+, and Si_n^- clusters in their equilibrium structure. Numerical data for the cohesion as well as the band structure and repulsive part of E_{coh} are summarized in Table I. The charged clusters should correspond to experimental conditions. We first note that the TB and LDA results follow the same trend for the cohesive energy of neutral clusters. Quantitative differences exist, both in relative stabilities as well as in equilibrium geometries which we will discuss below. Due to the similarity of the cohesion curves for neutral and charged Si_n clusters, we restrict most of our studies to neutral clusters.

The equilibrium structures of Si_n clusters up to a size $n=10$ are shown in Fig. 4. Si_2 is reproduced exactly in the TB model, by construction of the Hamiltonian. However, it is underbound in the LDA calculation.[22] Si_3 has an opening angle of $\approx 80°$, due to a Jahn-Teller distortion, and agrees with the singlet state found in independent calculations.[23,24] Si_4 is a flat rhombus with a side length of 2.3 Å and a diagonal of 2.4 Å. (The equilibrium TB values are ~ 0.1 Å longer.) A relaxed tetrahedron is less favorable in energy by ~ 0.5 eV/atom. The most stable structure for Si_5 is a "squashed" trigonal bipyramid. The basis triangle has a side length of 3.1 Å; the bonds between its corners and the caps are 2.4 Å long. We also find a metastable "pointed" geometry with a base length of 2.3 Å and the cap-to-base bond length of 2.3 Å. The equilibrium structure of Si_6 is a distorted octahedron. The side length of the square base is 2.6 Å (2.8 Å in TB) and the cap bond length is 2.3 Å (2.5 Å in TB). This geometry is more stable by 0.6 eV/atom (0.7 eV/atom in TB) than the relaxed sixfold ring,[5] a bulk fragment, also shown in Fig. 4. The specially stable octahedron structure serves as a building block for Si_n clusters up to $n=14$. These are obtained by decorating the sides with tetrahedron caps in such a way that the mutual adatom distances are maximum. On the basis of our total-energy calculations, different atomic arrangements led to higher energies. These were, e.g., two twisted squares for Si_8 and the same structure decorated by a cap for Si_9, which in

TABLE I. LDA and TB results for the cohesive energy per atom E_{coh}/n of Si_n clusters. For TB the band-structure part E_{BS}^{TB}/n and the repulsive part E_R^{TB}/n of the cohesion are also given, as well as the average number n_b/n of nearest-neighbor bonds.

Cluster size n	LDA E_{coh}/n (eV)	TB E_{coh}/n (eV)	TB E_{BS}/n (eV)	TB E_R/n (eV)	TB n_b/n
2	−0.6	−1.5	−4.9	3.4	0.50
3	−2.1	−2.3	−6.9	4.6	1.00
4	−2.8	−3.1	−8.4	5.3	1.25
5	−3.3	−3.0	−8.7	5.7	1.80
6	−3.5	−3.4	−9.4	6.0	2.00
7	−3.4	−3.5	−9.7	6.2	2.14
8	−3.3	−3.5	−9.7	6.2	2.25
9	−3.5	−3.5	−9.5	6.0	2.22
10	−4.0	−3.6	−9.8	6.2	2.40
11	−3.8	−3.9	−10.3	6.4	2.45
∞	−5.1	−4.6	−12.6	8.0	2.00

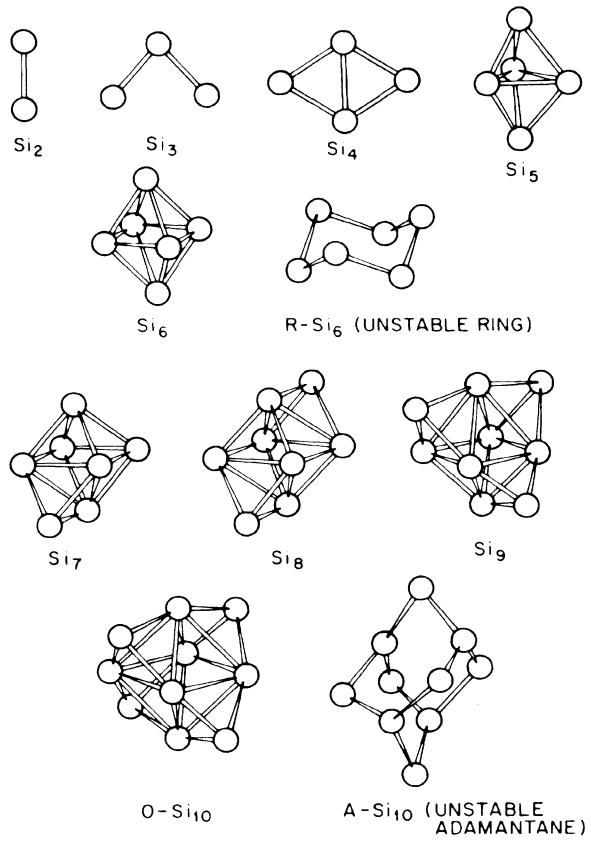

FIG. 4. Ball and stick models for calculated equilibrium structures of small Si_n clusters. The connections correspond to nearest-neighbor bonds. Also shown are the (metastable) crystalline fragments for $n=6$ and 10.

TB turned out to be unstable by 0.18 eV and 0.04 eV, respectively, with respect to the octahedron-based structures. The equilibrium Si_{10} cluster (O-Si_{10}) of four-capped octahedron with a side length of 2.5 Å (3.1 Å in TB) and a cap bond length of 2.3 Å (2.4 Å in TB). This structure is more stable by ≈ 0.9 eV/atom (0.8 eV/atom in TB) than the adamantane cage (A-Si_{10}), a building block of the silicon crystal in the diamond structure. These structures, both shown in Fig. 4, are topologically connected, as will be discussed later on. Surfaces of constant charge density, presented in Fig. 5, show the differences in the bonding type between the more stable octahedron and the adamantane structure of Si_{10}. A structure consisting of two twisted squares on top of each other, each decorated by a cap, is found slightly unstable within LDA, while within TB it is favored by 0.3 eV/atom with respect to the "best" octahedron-based structure. Beyond $n=10$, additional adatoms unfavorably overcoordinate the basic octahedron and do not further increase the binding energy per atom. These results for the Si_n clusters agree well with recent quantum-chemical calculations where available.[11–13]

Comparing equilibrium TB and LDA structures, we find that TB tends to exaggerate bond lengths by typically 0.1–0.2 Å. This effect is more pronounced in larger clusters. For highly coordinated sites, the pairwise repulsion $E_r(d)$, obtained from Si_2, shows too strong a distance dependence beyond the equilibrium distance. Equilibrium geometries can be strongly improved within the TB formalism, if $E_r(d)$ in Eq. (2.6) is reduced for large d, as can, e.g., be done by multiplying it by a smooth function:

$$E_r(d)=E_r(d)(\exp[(r-r_F)/a_F]+1)^{-1}\ , \tag{3.3}$$

where r_F and a_F are adjustable constants. Choosing r_F larger than the equilibrium bond length d_{eq} guarantees very little change in the energies for nearest-neighbor distances $d \lesssim d_{eq}$, smaller $E_r(d)$ for $d > d_{eq}$, and the correct asymptotic behavior. a_F and r_F were obtained by reproducing LDA results for both metastable states of Si_5 and Si_{10}. The best fit yielded $a_F=4$ Å and $r_F=7$Å. To reproduce the Si_2 and bulk Si data, the constants in the bond-number-dependent term had also to be modified to $\psi_1=0.350$ eV, $\psi_2=0.407$ eV, and $\psi_3=-1.186$ eV. Our experience with the TB Hamiltonian shows that the calculated types of equilibrium geometries are independent of the exact ψ_1 values and of small modifications of the repulsive terms. In order to keep the TB model as transparent as possible, we have *not* used the form (3.3) for the repulsion in the results presented in this paper.

As mentioned before, the adamantane structure of Si_{10} is topologically connected to the octahedron structure and can be obtained by moving the octahedron atoms at $(\pm r_0,0,0)$, $(0,\pm r_0,0)$, and $(0,0,\pm r_0)$ outwards by ≈ 0.9 Å and the tetrahedron atoms at $(r_t,\pm r_t,\mp r_t)$ and $(-r_t,\pm r_t,\pm r_t)$ inwards by about the same distance. Results of total-energy calculations for this transition are shown in Fig. 6. In Fig. 6(a) the TB total energy is given as a function of r_0 and r_t for a nearest-neighbor bond map corresponding to an adamantane structure; in Fig. 6(b) the TB total-energy surface is given for an octahedron nearest-neighbor bond map. It is interesting to note that despite the different connectivities of these structures, the A-nn map shows an energy minimum near an O structure and vice versa. As can be seen in Fig. 6(c), which summarizes LDA and TB results for the $A \rightarrow 0$ transformation along the minimum-energy path, the activation barrier of ≈ 0.1 eV/atom is quite small when compared with the energy difference $\Delta E \approx 0.9$ eV between these structures. The TB results, given by a dashed line, are in good qualitative agreement with the LDA results.

In order to find general rules for the stability and equilibrium structures of small Si_n clusters, we investigated the nature of the highest occupied (HOMO) and lowest unoccupied (LUMO) molecular orbitals as well as the gap which separates them. The results are given in Table I. Within our TB model, an orbital has been called bonding (B) if it increased in energy upon cluster expansion, antibonding (A) if it decreased in energy, and nonbonding (N) if its energy level did not change substantially. For the ease of comparison, LDA and TB gap energies have also been plotted as a function of cluster size in Fig. 7. We note that especially stable structures for $n=6$ and 10 in LDA show large semiconducting gaps and have a bonding HOMO and a non- or antibonding LUMO.

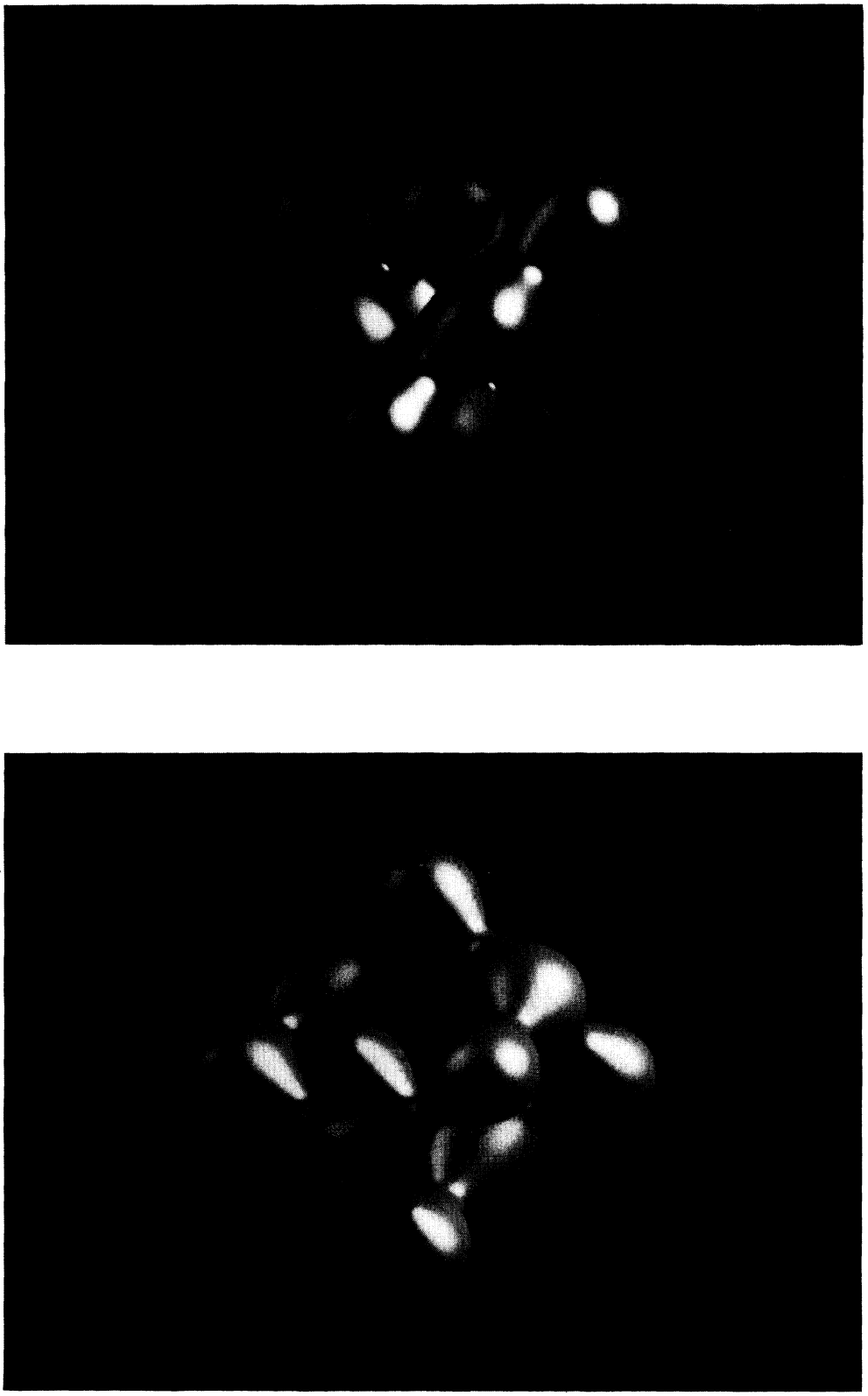

FIG. 5. A "view" of constant valence charge density surfaces for the metastable adamantane (bottom) and stable octahedron (top) structures of Si_{10}.

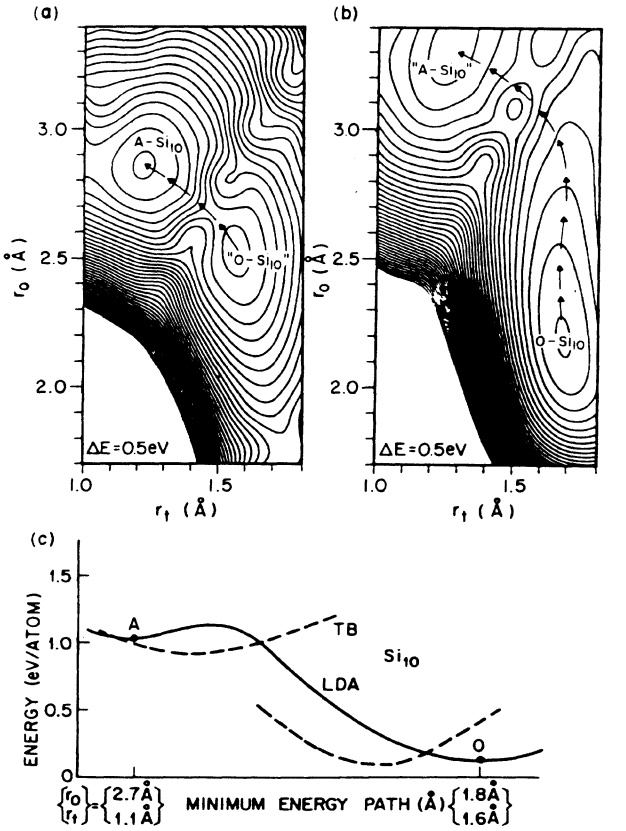

FIG. 6. Contour plots of tight-binding total-energy surfaces for Si_{10} as a function of atomic coordinates r_0 and r_t as defined in the text. The plots correspond to the nearest-neighbor maps of (a) adamantane (A)-Si_{10} and (b) octahedron (O)-Si_{10}. The equidistant contours are separated by 0.2 eV. Results of the LDA calculation for the A-$Si_{10}\rightarrow O$-Si_{10} transition along the minimum-energy path are given in (c) (solid line) and are compared to the tight-binding results (dashed lines).

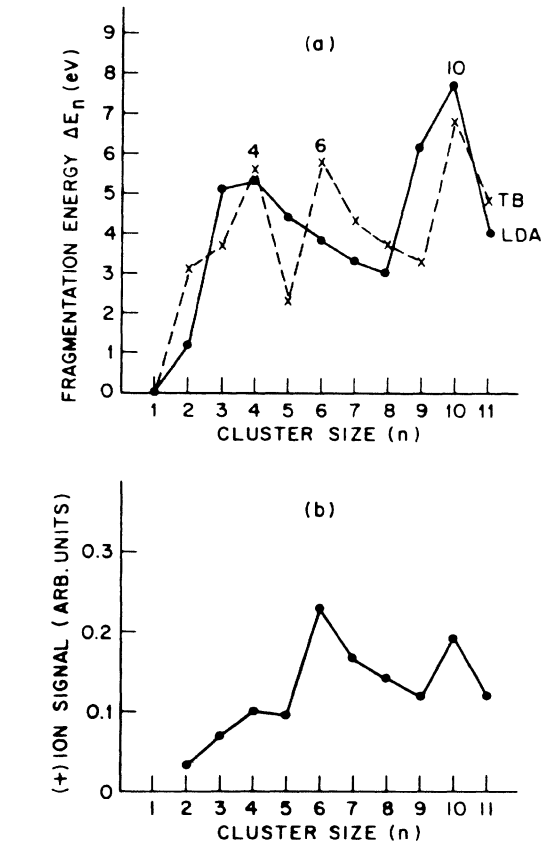

FIG. 8. (a) Fragmentation energy $\Delta E_n \equiv E_{\rm coh}(Si_{n-1}) - E_{\rm coh}(Si_n)$ as a function of cluster size n. The LDA results are given by the solid line, the TB results by the dashed line. (b) Typical Si_n^+ fragmentation mass spectrum as given in Ref. 5.

In order to compare our result to experimentally observed fragmentation spectra,[5] in Fig. 8(a) we show the fragmentation energy ΔE_n, which here is defined by

$$\Delta E_n = E_{\rm coh}(Si_{n-1}) - E_{\rm coh}(Si_n) \tag{3.4}$$

and (up to a constant) corresponds to the energy involved in removing one Si atom from a Si_n cluster. The pronounced maxima of ΔE_n for $n=6$ and 10 correspond to the observed abundant cluster sizes shown in Fig. 8(b).

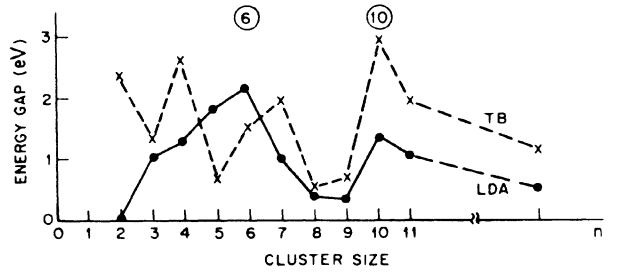

FIG. 7. Energy gap between the highest occupied and the lowest unoccupied cluster orbitals as a function of Si_n cluster size. Local-density functional results (solid line) and tight-binding results (dashed line) are shown.

Since the structures of Si_6 and Si_{10} are quite different from the crystal fragments of corresponding size, it is an important question, at which critical size $n^{\rm crit}$ a crossover occurs between compact and open crystallike structures. It seems plausible to assume that surface atoms tend to reduce their number of dangling bonds by assuming close-packed structures, while for the fully coordinated bulk atoms a transition to more compact structures is energetically unfavorable. We can roughly estimate $n^{\rm crit}$ by comparing energies of Si_n clusters in an open (diamond) and in a compact (bcc) structure,

$$\Delta E(n) = E_{\rm coh}(\text{open } Si_n) - E_{\rm coh}(\text{compact } Si_n)\ . \tag{3.5}$$

and using

$$\Delta E(n^{\rm crit}) = 0 \tag{3.6}$$

as the transition criterion. Distinguishing n_s surface atoms from $(n-n_s)$ bulk atoms in a Si_n cluster, we obtain

$$\Delta E(n) = n_s \Delta E_s + (n-n_s)\Delta E_b\ , \tag{3.7}$$

where

$$\Delta E_s = E_{\mathrm{coh},s}(\text{open Si}) - E_{\mathrm{coh},s}(\text{compact Si}) \tag{3.8a}$$

and

$$\Delta E_b = E_{\mathrm{coh},b}(\text{open Si}) - E_{\mathrm{coh},b}(\text{compact Si}) \tag{3.8b}$$

are assumed essentially independent of the cluster structure. Here, $E_{\mathrm{coh},s}$ and $E_{\mathrm{coh},b}$ are binding energies of surface and bulk atoms, respectively. Equations (3.6) and (3.7) finally give as condition for the structural transition

$$\frac{n_s^{\mathrm{crit}}}{n^{\mathrm{crit}}} = \frac{\Delta E_b}{\Delta E_b - \Delta E_s} \ . \tag{3.9}$$

Since in small clusters, such as Si_{10}, virtually all atoms are suface atoms, we can estimate ΔE_s from

$$\Delta E_s \approx \tfrac{1}{10} E_{\mathrm{coh}}(A\text{-}Si_{10}) - \tfrac{1}{10} E_{\mathrm{coh}}(O\text{-}Si_{10}) \ . \tag{3.10}$$

The result of our calculation yields $\Delta E_s = -0.9$ eV. Previous calculations[9] for bulk diamond and bcc Si give $\Delta E_b = +0.4$ eV. Inserting these values into Eq. (3.10) we get $n_s^{\mathrm{crit}}/n^{\mathrm{crit}} = 0.3$. The number of surface atoms n_s in clusters of n atoms can be estimated from geometrical considerations. Let us consider spherical clusters of radius R, consisting of "cubic" atoms with a cube length r and $R/r = m$, the number of shells. Then,

$$\frac{n_s}{n} = \frac{3}{m} - \frac{3}{m^2} + \frac{1}{m^3} \tag{3.11a}$$

and

$$n = \tfrac{4}{3}\pi m^3 \ . \tag{3.11b}$$

For large clusters, $R/r \gg 1$ and the terms of the order $1/m^2$ and $1/m^3$ can be neglected. Then, we obtain

$$n \approx \frac{36\pi}{(n_s/n)^3} \ . \tag{3.12}$$

Using $n_s/n = 0.3$ we obtain for the critical cluster site $n^{\mathrm{crit}} = 4200$ atoms, which is of course, a very rough estimate. It is interesting to note that a very similar argument, applied to clusters of transition metals with a bulk bcc structure, leads to similar critical cluster sizes for the fcc→bcc transition.[25] Small deviations in $n_s^{\mathrm{crit}}/n^{\mathrm{crit}}$ and additional correction terms will probably reduce n^{crit} and lead to critical cluster sites of $10^2 - 10^3$ atoms for the transition form compact to open crystal structures in silicon clusters.

IV. DISCUSSION

The use of a parametrized TB Hamiltonian for determining equilibrium structures seems reasonable in view of the large dimensionality of the configurational space and the small amount of computer time involved in those calculations. The energy evaluation in TB, including forces, was ~500 times faster than within LDA. Also, the results of the TB calculations gave more reliable structures than a comparable scheme using an optimized form of two- and three-body potentials.[26] The determination of the parameters, used in the TB Hamiltonian, is, however, not unique. As can be seen in Fig. 1, the TB single-site energies and hopping integrals give a relatively good fit of the valence (but not the conduction) band in Si. To improve results for other materials such as carbon, we select optimized electronic parameters from fits of all bands of different prototype structures.[27]

It has been shown in the last section that both structural and electronic properties of small Si clusters are strongly different from bulk crystal fragments. A Mulliken population analysis yielded an electronic configuration very close to s^2p^2 for all clusters studied here, in contrast to the sp^3 configuration in the crystal. A slightly decreasing population of s states from 1.95 electrons in Si_2 to 1.7–1.9 electrons in Si_{10} shows the correct trend towards bulk configuration, but the absolute change is very small and supports our finding of very large cluster sizes necessary for a transition to bulk behavior. In large enough clusters with a considerable portion of fully coordinated atoms, these bulklike atoms with a sp^3 configuration, which prefer open crystal structures, will reverse the close-packing tendency imposed on the cluster by the surface atoms with a s^2p^2 configuration.

The results of our study indicate a strong interplay of the electronic and geometric structure in small Si (or more generally semiconductor) clusters. This behavior is quite different from both simple-metal clusters, where the electronic structure does not strongly depend on atomic positions, and from rare-gas clusters, where the equilibrium structure is rather independent from electronic states. Charging a Si_n cluster can both induce or suppress a Jahn-Teller distortion. The same effect can occur due to level crossing upon bond-length changes.

The latter effect has been studied for the transition from the metastable "pointed" (P) to the "squashed" (S) geometry of Si_5. During this transition, a bonding orbital, which is a hybrid of p_z states on the base and p_z and s states on the caps and which is occupied in P-Si_5, crosses the HOMO of P-Si_5 near the saddle point of the total energy. For P-Si_5, the HOMO is doubly degenerate and occupied by only two electrons, which gives rise to a Jahn-Teller instability. Near the S-Si_5 side of the transition path, the crossing orbital transfers both its electrons to the Si_5 HOMO thus removing the Jahn-Teller instability for S-Si_5. From the Mulliken population analysis, the net charges on the cap decrease considerably from $q_c = -0.20$ in P-Si_5 to $q_c = -0.11$ in the more symmetric S-Si_5.

A similar TB analysis has been performed for the adamantane (A) to the decorated octahedron (O) transition of Si_{10} shown in Fig. 6. However, the limitations of the TB Hamiltonian, which depends on the nearest-neighbors bond map, manifest themselves in this case, since the connectivities of A-Si_{10} and O-Si_{10} are different. Nevertheless, it is interesting to find in Figs. 6(a) and 6(b) local-energy minima corresponding to A and O structures for *both* nearest-neighbor maps. Both maps also give a consistent picture of the orbital behavior during this transition, which is similar to that observed in Si_5. In A-Si_{10} the three-fold-degenerate HOMO, which is a hybrid orbital involving s and p states on all atoms, is occupied by only two electrons, which leads to a Jahn-Teller distortion. Near the energy barrier for the transition to O-Si_{10}, shown in Fig. 6(c), a previously occupied doubly degenerate orbital crosses the HOMO of A-Si_{10}, becoming the LUMO of O-Si_{10} and stabilizing this structure against

Jahn-Teller distortions. This orbital involves p states on the cap atoms, which hybridize with s and p orbitals (only those pointing out of the cubic cell) on the octahedron atoms. During this transition, the net charge on the threefold coordinated atoms $q_T = -0.24$ in the A structure strongly decreases in magnitude and changes sign to $q_T = +0.06$ for the cap atoms in the more stable O structure. In the course of this transition, the semiconducting gap of 0.7 eV for A-Si_{10} first closes near the barrier and then opens to its large O-Si_{10} value of 2.9 eV (TB value).

In order to understand the structure in the stability curves of Si_n, Si_n^+, and Si_n^- clusters given in Fig. 3, we investigated the size dependence of the different energy terms constituting the TB cohesive energy. The average number of bonds per atom as well as the repulsive energy per atom turned out to be rather structureless. On the other hand, we found that the structure of the cohesive energy curve coincided quite well with that of the band-structure energy. This feature is well known[28] and is used to further analyze our results.

To understand the trends in $E_{coh}(Si_n)$, in Fig. 7 and Table II we show LDA and TB results for the semiconducting gap between the HOMO and LUMO. While LDA tends to underestimate gap energies, we still expect to obtain correct trends, which is confirmed also by comparing the LDA and TB curves. We find that structures with large gaps for $n = 4$, 6, and 10 correspond to especially stable cluster sizes.

We further expect a large stability for structures with a bonding HOMO and an antibonding LUMO. In Table II we also tabulate the characters of these orbitals and, based on the above argument, indeed find Si_6 and Si_{10} stable when compared to clusters of neighboring sizes.

It is interesting to draw general conclusions about the Si cluster growth and the stable geometries on the basis of our results. We speculate that geometries involving bond angles larger than 90°, such as in Si_4 and Si_6, should favor the sp hybridization and open the semiconducting gap, hence stabilizing the structures. On the other hand, the octahedron structure of Si_6 also corresponds to the most close-packed arrangement possible. The close-packing argument leads to octahedron-based structures with essentially unchanged bond lengths, whose sides are decorated by caps. The cap bond lengths are smaller due to the low coordination of the cap atoms, so that the cap atoms significantly stabilize the basic octahedron. For $n > 10$, however, the overcoordination of the octahedron atoms turns out to be energetically unfavorable,[29] which leaves O-Si_{10} as an especially stable structure. A-Si_{10}, on the other hand, turns out to be very unstable, mainly due to the low coordination of all of its atoms.

In Fig. 8(a) we investigated the stability of Si_n clusters with respect to evaporation of isolated Si atoms. This fragmentation process is least energy intensive and should occur most frequently, the exception being emission of very stable fragments such as Si_6 or Si_{10} for larger clusters. We find an agreement between cluster sizes which are stable towards fragmentation and experimentally observed fragmentation mass spectra of Si_n^+ reproduced in Fig. 8(b). This close agreement is nontrivial in view of the fact that the experimental conditions need not be close to equilibrium and also since we did not investigate charged clusters with the same precision as the neutral ones.

In clusters of germanium, which shows a similar type of bonding as silicon, we expect very similar results for the equilibrium structures and magic numbers. This is supported by recent calculations[30] of Ge_2—Ge_6 and by observed abundancies in Ge_n^+ mass spectra.[31] On the other hand, very different equilibrium structures and magic numbers are expected in carbon due to the significance of π bonding in this system.[32]

In conclusion, we studied the structural stability and electronic properties of Si_n, Si_n^+, and Si_n^+, clusters up to $n = 14$. A tight-binding formalism has been used to find stable structures, which were further investigated in the density functional formalism. No open structures or fragments were found for these cluster sizes. A transition to open structures in expected to occur at cluster sizes $n \approx 10^2 - 10^3$. The most stable structures for $n = 4$, 6, and 10 show a large semiconducting gap between highest occupied and lowest unoccupied states. These sizes coincide with observed abundancies in the mass spectra of Si_n clusters.

TABLE II. LDA and TB results for the gap energy E_{gap} between the highest occupied (HOMO) and lowest unoccupied (LUMO) molecular orbitals, as well as their bonding behavior. B denotes bonding-, A denotes antibonding-, and N nonbonding-type orbital.

Cluster size n	E_{gap}^{LDA} (eV)	E_{gap}^{TB} (eV)	HOMO type	LUMO type
2	0.0	0.0	B	A
3	0.9	1.3	B	A
4	1.1	2.6	B	N
5	1.8	0.7	B	B
6	2.1	1.5	B	N
7	0.9	2.0	B	N
8	0.4	0.5	N	N
9	0.4	0.7	B	N
10	1.2	2.9	B	A
11	0.9	2.0	N	A
∞	0.6	1.1	B	A

ACKNOWLEDGMENTS

We acknowledge useful discussions with R. R. Freeman, L. A. Bloomfield, K. Raghavachari, D. R. Hamann, J. C. Phillips, J. J. Joannopoulos, and G. Pacchioni. We thank D. Mitchell for generating the computer plots of Fig. 5. One of us (D.T.) acknowledges the hospitality of the AT&T Bell Laboratories and financial support of the Deutsche Forschungsgemeinschaft (Sonderforschungsbereich 6) as well as the Stifterverband für die Deutsche Wissenschaft. D.T. was further supported by the Director, Office of Energy Research, Office of Basic Sciences, Material Sciences Division of the U.S. Department of Energy under Contract No. DE-AC03-76SF00098. This report was completed during a stay at the Aspen Physics Institute whose hospitality we acknowledge.

[1]W. Brown, R. R. Freeman, K. Raghavachari, and M. Schlüter, Science **235**, 860 (1987); M. Y. Chou and M. L. Cohen (unpublished). For a recent compendium of papers see Surf. Sci. **156**, (1985), Pts. 1 and 2.
[2]M. F. Geuski, M. D. Morse, and R. E. Smalley, J. Chem. Phys. **82**, 590 (1985).
[3]G. Apai, J. F. Hamilton, J. Stöhr, and A. Thompson, Phys. Rev. Lett. **43**, 165 (1979).
[4]O. Echt, K. Sattler, and E. Recknagel, Phys. Rev. Lett. **47**, 1121 (1981).
[5]L. A. Bloomfield, R. R. Freeman, and W. L. Brown, Phys. Rev. Lett. **54**, 2246 (1985).
[6]R. Rosetti, R. Hull, J. M. Gibson, and L. E. Brus, J. Chem. Phys. **82**, 552 (1983).
[7]C. J. Sandroff, D. M. Hwang, and W. H. Chang, Phys. Rev. B **33**, 5953 (1986).
[8]W. D. Knight, K. Clemenger, W. A. de Heer, W. A. Saunders, M. Y. Chou, and M. L. Cohen, Phys. Rev. Lett. **52**, 2141 (1984).
[9]M. T. Yin and M. L. Cohen, Phys. Rev. Lett. **45**, 1004 (1985).
[10]D. Tománek and M. A. Schlüter, Phys. Rev. Lett. **56**, 1055 (1986).
[11]K. Raghavachari and V. Logovinsky, Phys. Rev. Lett. **55**, 2853 (1985).
[12]G. Pacchioni and J. Koutecký, J. Chem. Phys. **84**, 3301 (1986).
[13]R. Mosseri and J. P. Gaspard, J. Phys. (Paris) Colloq. **42**, C4-245 (1981).
[14]M. Schluter and L. J. Sham, Phys. Today **35**(2), 30 (1982).
[15]D. J. Chadi, Phys. Rev. B **29**, 785 (1984).
[16]P. Hohenberg and W. Kohn, Phys. Rev. **136**, B864 (1964); W. Kohn and L. J. Sham, Phys. Rev. **140**, A1133 (1965).
[17]J. C. Slater and G. F. Koster, Phys. Rev. **94**, 1498 (1954).
[18]K. Raghavachari (private communication).
[19]D. R. Hamann, M. Schlüter, and C. Chiang, Phys. Rev. Lett. **43**, 1494 (1979).
[20]D. M. Ceperly and B. I. Alder, Phys. Rev. Lett. **45**, 566 (1980).
[21]B. Holland, H. S. Greenside, and M. Schlüter, Phys. Status Solidi **126**, 511 (1984).
[22]While LDA generally tends to overbind, the limited basis size used here will tend to decrease the cohesion especially of very small clusters.
[23]G. H. F. Dierksen, N. E. Grüner, J. Oddershede, and J. R. Sabin, Chem. Phys. Lett. **117**, 24 (1985); R. S. Grev and H. F. Schäfer, *ibid.* **119**, 111 (1985).
[24]K. Raghavachari, J. Chem. Phys. **83**, 3250 (1985); R. O. Jones, Phys. Rev. A **32**, 2589 (1985).
[25]D. Tománek, S. Mukherjee, and K. H. Bennemann, Phys. Rev. B **28**, 665 (1983); **29**, 1076(E) (1984).
[26]R. Biswas and D. R. Hamann, Phys. Rev. B **34**, 895 (1986).
[27]D. Tománek and M. A. Schlüter (unpublished).
[28]J. C. Slater, *Quantum Theory of Molecules and Solids* (McGraw-Hill, New York, 1963), Vol. 1.
[29]M. R. Hoare and P. Pal, Adv. Phys. **20**, 161 (1971).
[30]G. Pacchioni and J. Kontecký, Ber. Bunsenges. Phys. Chem. **88**, 242 (1984).
[31]L. A. Bloomfield (private communication).
[32]J. Bernholc and J. C. Phillips, Phys. Rev. B **23**, 7395 (1986); E. A. Rohlfing, D. M. Cox, and A. Kaldor, J. Chem. Phys. **81**, 3322 (1984); H. W. Kroto, J. R. Heath, S. C. O'Brien, R. F. Curl, and R. E. Smalley, Nature **318**, 162 (1985); R. C. Haddon, L. E. Brus, and K. Raghavachari, Chem. Phys. Lett. **125**, 459 (1986); K. Raghavachari and J. S. Binkley, *ibid.* **131**, 165 (1986).

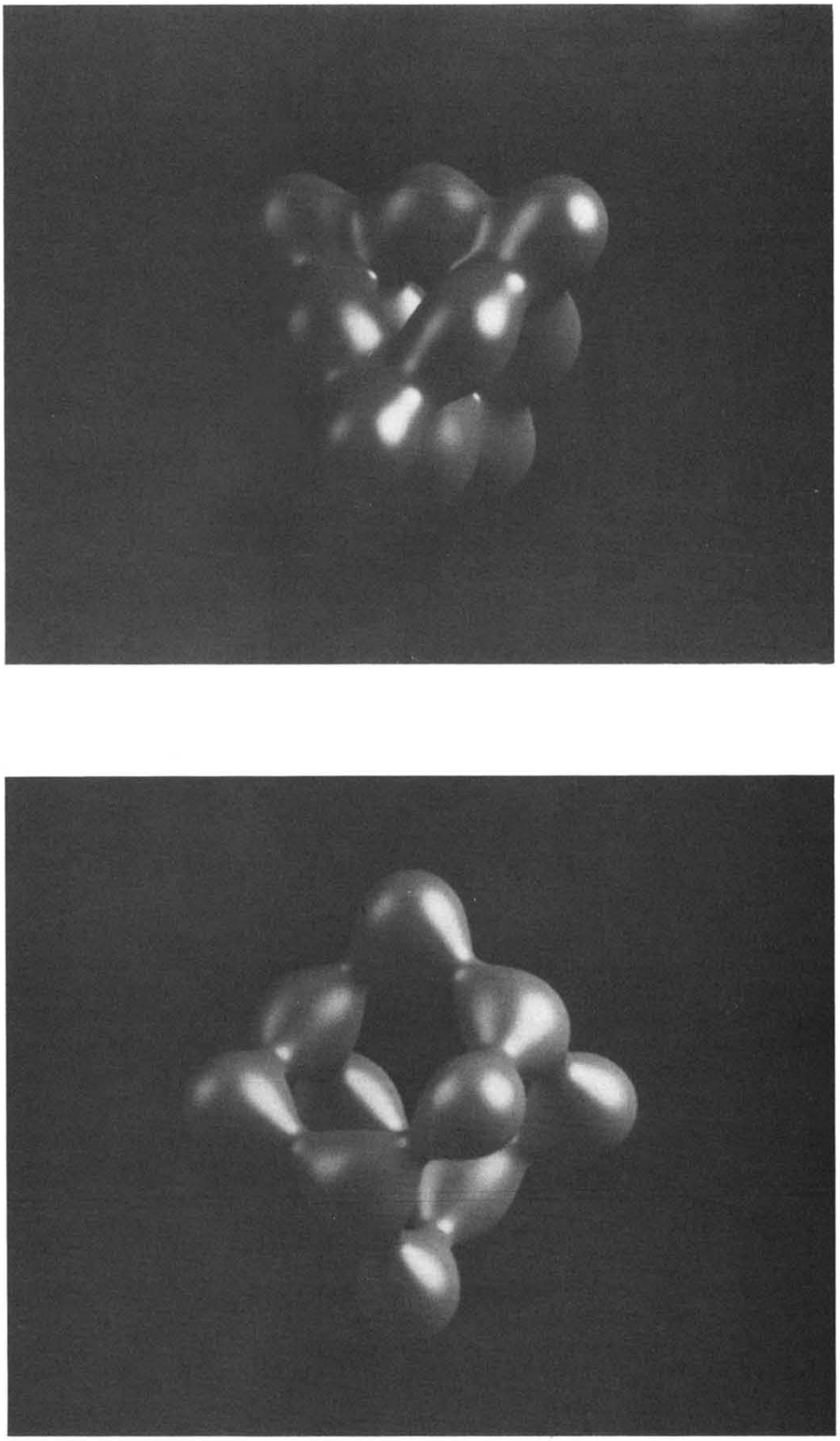

FIG. 5. A "view" of constant valence charge density surfaces for the metastable adamantane (bottom) and stable octahedron (top) structures of Si_{10}.